

Trastuzumab-Resistant Cells Rely on a HER2-PI3K-FoxO-Survivin Axis and Are Sensitive to PI3K Inhibitors

Anindita Chakrabarty¹, Neil E. Bholra², Cammie Sutton², Ritwik Ghosh², María Gabriela Kuba³, Bhuvanesh Dave⁵, Jenny C. Chang⁵, and Carlos L. Arteaga^{1,2,4}

Abstract

The antibody trastuzumab is approved for treatment of patients with HER2 (ERBB2)-overexpressing breast cancer. A significant fraction of these tumors are either intrinsically resistant or acquire resistance rendering the drug ineffective. The development of resistance has been attributed to failure of the antibody to inhibit phosphoinositide 3-kinase (PI3K), which is activated by the HER2 network. Herein, we examined the effects of PI3K blockade in trastuzumab-resistant breast cancer cell lines. Treatment with the pan-PI3K inhibitor XL147 and trastuzumab reduced proliferation and pAKT levels, triggering apoptosis of trastuzumab-resistant cells. Compared with XL147 alone, the combination exhibited a superior antitumor effect against trastuzumab-resistant tumor xenografts. Furthermore, treatment with XL147 and trastuzumab reduced the cancer stem-cell (CSC) fraction within trastuzumab-resistant cells both *in vitro* and *in vivo*. These effects were associated with FoxO-mediated inhibition of transcription of the antiapoptosis gene survivin (*BIRC5*) and the CSC-associated cytokine interleukin-8. RNA interference-mediated or pharmacologic inhibition of survivin restored sensitivity to trastuzumab in resistant cells. In a cohort of patients with HER2-overexpressing breast cancer treated with trastuzumab, higher pretreatment tumor levels of survivin RNA correlated with poor response to therapy. Together, our results suggest that survivin blockade is required for therapeutic responses to trastuzumab and that by combining trastuzumab and PI3K inhibitors, CSCs can be reduced within HER2⁺ tumors, potentially preventing acquired resistance to anti-HER2 therapy. *Cancer Res*; 73(3); 1190–200. ©2012 AACR.

Introduction

The *HER2* oncogene encodes a transmembrane receptor tyrosine kinase (RTK) that is amplified in approximately 20% of invasive breast cancers (1). *HER2* gene amplification in breast cancer is associated with increased cell proliferation and motility, tumor invasion and metastasis, accelerated angiogenesis, decreased apoptosis, and resistance to anticancer therapy (2). This translates into shorter disease-free and overall survival in patients (3). In HER2-overexpressing cells, HER2 dimerizes with its coreceptor HER3 that, in turn, directly couples to the p85 regulatory subunit of phosphoinositide 3-kinase (PI3K) and activates the PI3K/AKT survival pathway (4–6).

Trastuzumab, a humanized antibody directed against the extracellular domain of the HER2 receptor, is approved for the

treatment of HER2-overexpressing breast cancer (7). Mechanisms of action of the antibody include endocytosis and down-regulation of HER2, inhibition of ligand-independent HER2-HER3 dimers with subsequent inhibition of PI3K/AKT, and induction of cell-cycle arrest and apoptosis. In addition, trastuzumab engages Fc receptor-expressing immune effector host cells to induce antibody-dependent, cell-mediated cytotoxicity (ADCC; reviewed in ref. 8).

Although patients with metastatic HER2⁺ breast cancer respond clinically to single-agent trastuzumab or in combination with chemotherapy, virtually all patients eventually adapt to the anti-HER2 therapy and progress (reviewed in ref. 9). One of the major proposed mechanisms of adaptation or resistance to trastuzumab involves aberrant activation of the PI3K/AKT pathway by (i) loss of the tumor suppressor *phosphatase and tensin homolog deleted on chromosome 10* (*PTEN*; ref. 10) and (ii) activating mutations in *PIK3CA*, the gene encoding the p110 α catalytic subunit of PI3K (11). The dependence of HER2-overexpressing breast cancer cells on the PI3K/AKT pathway together with several genetic and epigenetic alterations in the PI3K pathway associated with trastuzumab resistance suggest that early use of PI3K pathway inhibitors should be useful in preventing or delaying clinical resistance to trastuzumab. Indeed, several PI3K inhibitors have been shown to block growth of preclinical models of trastuzumab resistance (12, 13) and are currently the focus of clinical development in patients with breast cancers (reviewed in ref. 14).

Authors' Affiliations: Departments of ¹Cancer Biology, ²Medicine, ³Pathology, and ⁴Breast Cancer Research Program, Vanderbilt-Ingram Cancer Center, Vanderbilt University School of Medicine, Nashville, Tennessee; and ⁵Methodist Cancer Center, Methodist Hospital Research Institute, Houston, Texas

Note: Supplementary data for this article are available at Cancer Research Online (<http://cancerres.aacrjournals.org/>).

Corresponding Author: Carlos L. Arteaga, Division of Hematology-Oncology, VUMC, 2220 Pierce Avenue, 777 PRB, Nashville, TN 37232. Phone: 615-936-3524; Fax: 615-936-1790; E-mail: carlos.arteaga@vanderbilt.edu

doi: 10.1158/0008-5472.CAN-12-2440

©2012 American Association for Cancer Research.

In this study, we used breast cancer models of trastuzumab resistance with different modes of aberrant PI3K pathway activation to examine the effects of ATP-mimetic, small-molecule inhibitors of PI3K either alone or in combination with trastuzumab both *in vitro* and *in vivo*. Treatment with the pan-PI3K inhibitor XL147 (15) with or without trastuzumab reduced proliferation and pAKT levels and induced apoptosis of trastuzumab-resistant cells. The combination potently inhibited trastuzumab-resistant xenografts established in athymic mice. Treatment with XL147 alone or in combination with trastuzumab modulated the cancer stem cell (CSC) fraction, which has been causally associated with drug resistance and tumor recurrences (16). Pharmacologic and RNA interference (RNAi)-based approaches suggested this was, at least in part, due to derepression of FoxO-mediated transcription that, in turn, downregulated expression of interleukin (IL)-8 and the antiapoptosis protein survivin. Finally, in patients with HER2-overexpressing breast cancer treated with trastuzumab, higher pretreatment tumor levels of survivin RNA correlated with poor response to therapy. Taken together, these data suggest that (i) trastuzumab-resistant cells continue to rely on HER2-PI3K-FoxO-survivin axis for survival, and (ii) modulation of this axis with a combination of PI3K and HER2 inhibitors may abrogate or delay the development of resistance to anti-HER2 therapy.

Materials and Methods

Cell lines, reagents, inhibitors, plasmids, and viral vectors

All cell lines were from the American Tissue Culture Collection (ATCC), maintained in ATCC-recommended media plus 10% FBS (Gibco) and authenticated by short tandem repeat profiling using Sanger sequencing (March 2011). HR5 and HR6 cells were derived from previously described BT474 xenografts with acquired resistance to continuous treatment with trastuzumab (17). WST-1 reagent and Caspase-Glo 3/7 assay kit were obtained from Roche Applied Science and Promega Corporation, respectively. The following inhibitors were used: lapatinib and BEZ235 (LC Laboratories), BKM120 (Active Biochem), YM155 (Selleck Chemicals), trastuzumab (VUMC Pharmacy), and XL147 (Exelixis). The FHRE-Luc reporter plasmid (Addgene plasmid#1789) has been described previously (18). The *Renilla* Luc pRL-SV40 and human survivin cDNA-pJP1520 were obtained from Promega and Labome/DNASU plasmid repository, respectively. Retrovirus and stable cell line production were described previously (19). Adenoviruses encoding β -galactosidase/LacZ, non-phosphorylatable FKHL1/FoxO3(AAA) mutant and dominant-negative/dnFoxO3, both GFP-tagged, were from Vector Biolabs. Adenovirus infection was conducted as described previously (20).

Cell proliferation, immunoprecipitation, immunoblot analysis, RNA interference, and real-time quantitative PCR

These methods were conducted as described previously (21). Human FoxO1 and FoxO3a siRNAs were described previously (22). The p110 α , p110 β , and survivin siRNA duplexes were

obtained from Ambion and Cell Signaling Technology. Primers for quantitative PCR (qPCR) were obtained from Qiagen.

Mammosphere and aldehyde dehydrogenase assays

For mammosphere assay, 0.5×10^4 to 1×10^4 cells/well were seeded in 6-well Ultra-low attachment plates (Costar) in Dulbecco's Modified Eagles' Media (DMEM):F12 + 20 ng/mL EGF + $1 \times$ B-27 serum-free supplement (Invitrogen). Imaging and quantitation of colonies were done in GelCount colony counter (Oxford Optronix). Mammospheres were dissociated by trypsin digestion, and 1,000 cells/well were seeded in 6-well plates in IMEM/10% serum (Fig. 4J). Focus/colony formation was assessed 7 days later. Colonies were fixed and stained with methanol crystal violet and imaged. Aldehyde dehydrogenase (ALDH) assay was conducted with ALDEFLUOR kit (Stemcell Technologies) and subsequent fluorescence-activated cell-sorting (FACS) analysis in a 3 laser LSRII (BD Biosciences).

Dual luciferase reporter assay

Cells were transfected with 10 μ g FHRE-Luc (18) plus 100 ng pRL-SV40 with FuGENE 6 (Promega) and treated overnight with trastuzumab, XL147, or both. Dual luciferase assay was conducted with the Dual-Luciferase Reporter Assay System (Promega).

Proteome Profiler human angiogenesis and phospho-RTK arrays

Angiogenesis (ARY007) and pRTK (ARY001) arrays were conducted according to manufacturer's instructions (R&D Systems).

Xenograft studies

These were approved by the Institutional Animal Care Committee of Vanderbilt University (Nashville, TN). A 17 β -estradiol pellet (Innovative Research of America) was injected subcutaneously in the dorsum of 4- to 5-week-old athymic female mouse (Harlan Sprague Dawley, Inc.). Next day, HR6 cells ($\sim 3 \times 10^6$) mixed 1:1 with Matrigel (BD Biosciences) were injected s.c. into the right flank of each mouse. Tumor diameters were measured twice a week and volume in mm³ calculated by the formula: volume = width² \times length/2. Mice with ≥ 200 mm³ tumors were randomized to vehicle, trastuzumab (30 mg/kg twice a week intraperitoneally), XL147 (100 mg/kg daily *per os*), or combination treatments for 28 days. Immunostaining and histoscore (*H*-score) analysis of formalin-fixed tumor sections harvested on day 28 were conducted as described previously (22).

Results

Trastuzumab-resistant cells remain dependent on PI3K

We treated a panel of trastuzumab-resistant *HER2* gene-amplified human breast cancer cells with the pan-PI3K inhibitor XL147 (15) and the MEK inhibitor CI-1040 (23), either alone or in combination with trastuzumab. The HR5 and HR6 cell lines, derived from BT474 xenografts, grew in presence of trastuzumab *in vivo* and overexpress EGFR/HER3 ligands (17). The HCC1954 and SUM190 cell lines contain a mutation

in the catalytic domain (H1047R) of *PIK3CA* and HCC1569 cells are *PTEN*-null (22, 24). Treatment with XL147 + trastuzumab but not CI-1040 + trastuzumab inhibited monolayer (Fig. 1A) and 3-dimensional growth (Fig. 1B) in all resistant lines. CI-1040 alone was inactive against all cell lines, whereas growth of 3 of 5 resistant lines (HR5, HR6, and HCC1569) was inhibited by XL147, suggesting they depend on the PI3K/AKT pathway. The combination of XL147 and trastuzumab induced cell death and growth arrest as supported by immunoblot analysis of cleaved caspase-3 and PARP (apoptosis) and CDK inhibitor p27^{Kip1} (cell-cycle arrest; ref. Fig. 1C). This was further confirmed by enhanced caspase-3/7 activity following treatment with XL147 + trastuzumab compared with each inhibitor alone (Fig. 1D). The PI3K dependence of trastuzumab-resistant cells was also supported by siRNA-mediated knockdown of the p110 α and p110 β subunits of PI3K (Supplementary Fig. S1D). Compared with the cells transfected with control siRNA and treated with trastuzumab, knockdown of both p110 α and p110 β resulted in greater inhibition of cell growth in both monolayer and in 3-dimensional (Supplementary Fig. S1A and S1B) as well as

apoptosis measured by activation of caspase-3/7 (Supplementary Fig. S1C).

We next examined the effect of XL147, trastuzumab, and the combination on activated AKT, a main downstream target of PI3K (Fig. 2A). In all cell lines, treatment with XL147 alone or in combination with trastuzumab reduced pAKT^{S473} and pAKT^{T308} levels (Fig. 2A). Inhibition of PI3K/AKT is counteracted by compensatory feedback activation of RTKs, including HER3 (22, 25). In HER2-dependent breast cancer cells and xenografts, this compensation is reduced by cotreatment with trastuzumab or the HER2 tyrosine kinase inhibitor (TKI) lapatinib (22). To determine whether a similar phenomenon occurs in trastuzumab-resistant cells, we hybridized lysates of cells treated with XL147 \pm trastuzumab with arrays representing 42 different phosphorylated RTKs. The combination of XL147 + trastuzumab resulted in a modest reduction in pEGFR, pHER2, and pHER3 levels compared with XL147 alone (Fig. 2B; arrows).

In all 3 trastuzumab-resistant lines, treatment with both inhibitors reduced phosphorylation of VEGFR1 and/or

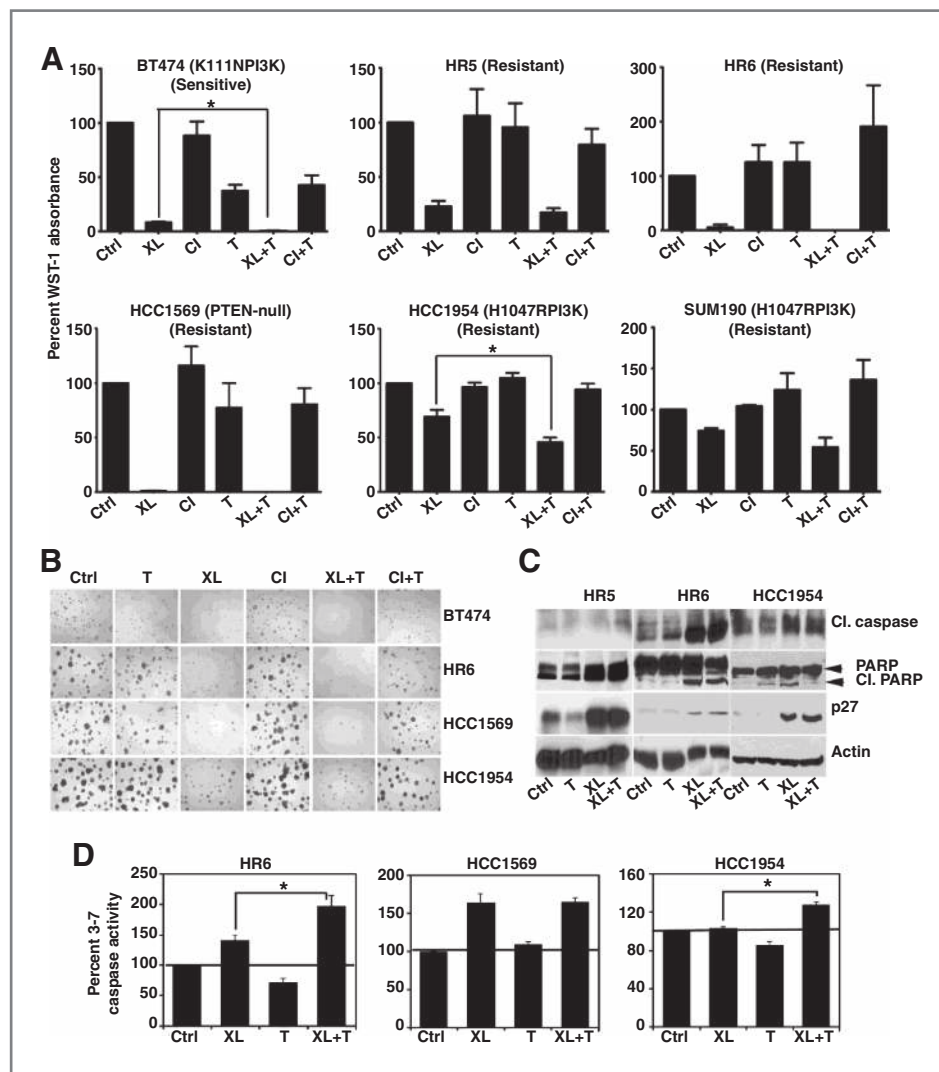
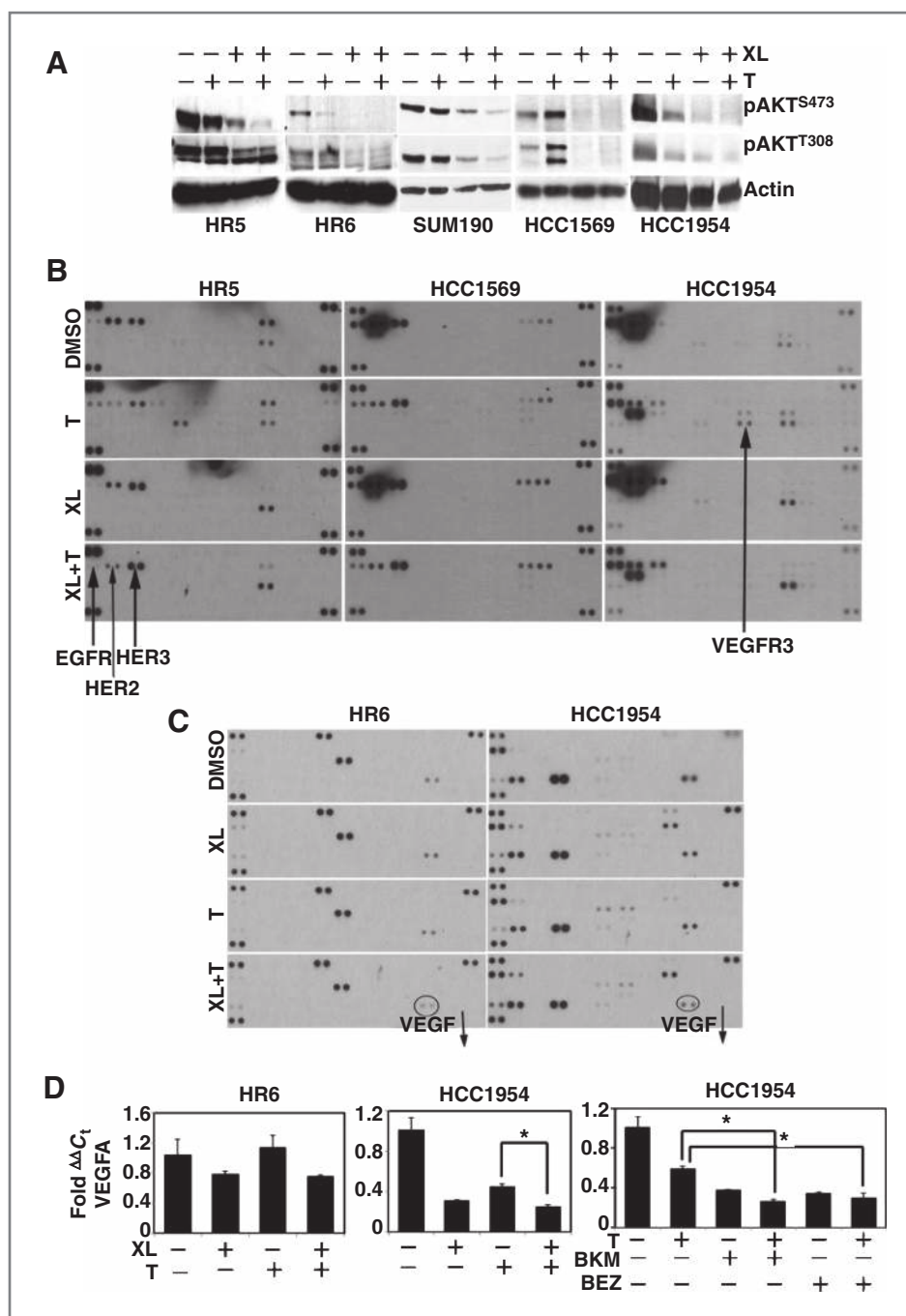


Figure 1. XL147 but not CI-1040 inhibits trastuzumab-resistant cells. **A**, breast cancer cell lines sensitive or resistant to trastuzumab (lesions in the PI3K pathway are indicated within parentheses on top of each panel) were treated with dimethyl sulfoxide (Ctrl), XL147 (6 μ mol/L), CI-1040 (0.5 μ mol/L), trastuzumab (10 μ g/mL) alone, or XL147 + trastuzumab and CI-1040 + trastuzumab for 5 days. Cell viability was measured by the WST-1 assay. Each bar represents mean \pm SE of 4 replicates. *, $P < 0.05$; paired t test. **B**, cells were grown in Matrigel with or without inhibitors as in **A** and photographed ($\times 4\times$ magnification) on day 11. **C**, cells were treated with or without XL147, trastuzumab, or both for 24 hours and harvested for immunoblot analysis. **D**, cells were treated with XL147 (6 μ mol/L), trastuzumab (10 μ g/mL), or both for 24 hours (HR5 and HR6) or 48 hours (HCC1569 and HCC1954) before conducting the Caspase-Glo 3/7 assay. Results were expressed as percent over dimethyl sulfoxide control (straight line is drawn at 100%). Each bar represents mean \pm SE of 8 replicates. *, $P < 0.05$; paired t test.

Figure 2. Combination therapy inhibits signal transduction and expression of angiogenic factors. **A** and **B**, cell lines were harvested after a 24-hour treatment with XL147 (6 $\mu\text{mol/L}$ HR5, HR6, SUM190, HCC1569 and 10 $\mu\text{mol/L}$ HCC1954), trastuzumab (10 $\mu\text{g/mL}$), or both inhibitors. **A**, cell lysates were subjected to immunoblot analysis with the indicated antibodies. **B**, cell lysates (500 μg) were hybridized with pRTK arrays. Arrows highlight pRTKs modulated by treatments indicated at the left. **C**, HR6 and HCC1954 cells were treated with dimethyl sulfoxide (DMSO), XL147, trastuzumab, or both as in **A**. Each lysate (500 μg) was hybridized with angiogenesis arrays. VEGF (circled) was downregulated following treatment with XL147 + trastuzumab. **D**, qRT-PCR for VEGFA mRNA in trastuzumab-resistant cells treated with DMSO, trastuzumab, XL147 or BKM120 (1 $\mu\text{mol/L}$), and BEZ235 (250 nmol/L), either alone or in the indicated combinations for 48 hours. Each bar represents mean \pm SE of triplicates. *, $P < 0.05$; paired t test.



VEGFR3 (Fig. 2B; longer exposure in Supplementary Fig. S2A). Related to this finding, trastuzumab has been shown to act as an antiangiogenic agent by affecting different proangiogenic proteins including VEGF and angiopoietin (26). Thus, we examined the effect of XL147 \pm trastuzumab on the expression of 55 angiogenic growth factors by hybridizing HR6 and HCC1954 cell lysates with protein arrays. In both cell lines, only the combination of XL147 + trastuzumab, but not each drug alone, reduced the expression of VEGF (Fig. 2C). Several other proangiogenic factors including angiopoietin-1 and -2,

IL-8, and Chemokine ligand-4 were also downregulated in a cell line-specific manner (longer exposure in Supplementary Fig. S2B and S2C). Of note, VEGF has a central role in breast cancer development and progression and its expression is regulated by the PI3K pathway (27). Real-time PCR with RNA from HR6 and HCC1954 cells showed a reduction in VEGFA RNA following treatment with XL147 alone or in a combination with trastuzumab (Fig. 2D). Similar data were obtained with the pan-PI3K inhibitor BKM120 (28) and the PI3K/mTOR inhibitor BEZ235 (29), either alone or in combination with trastuzumab

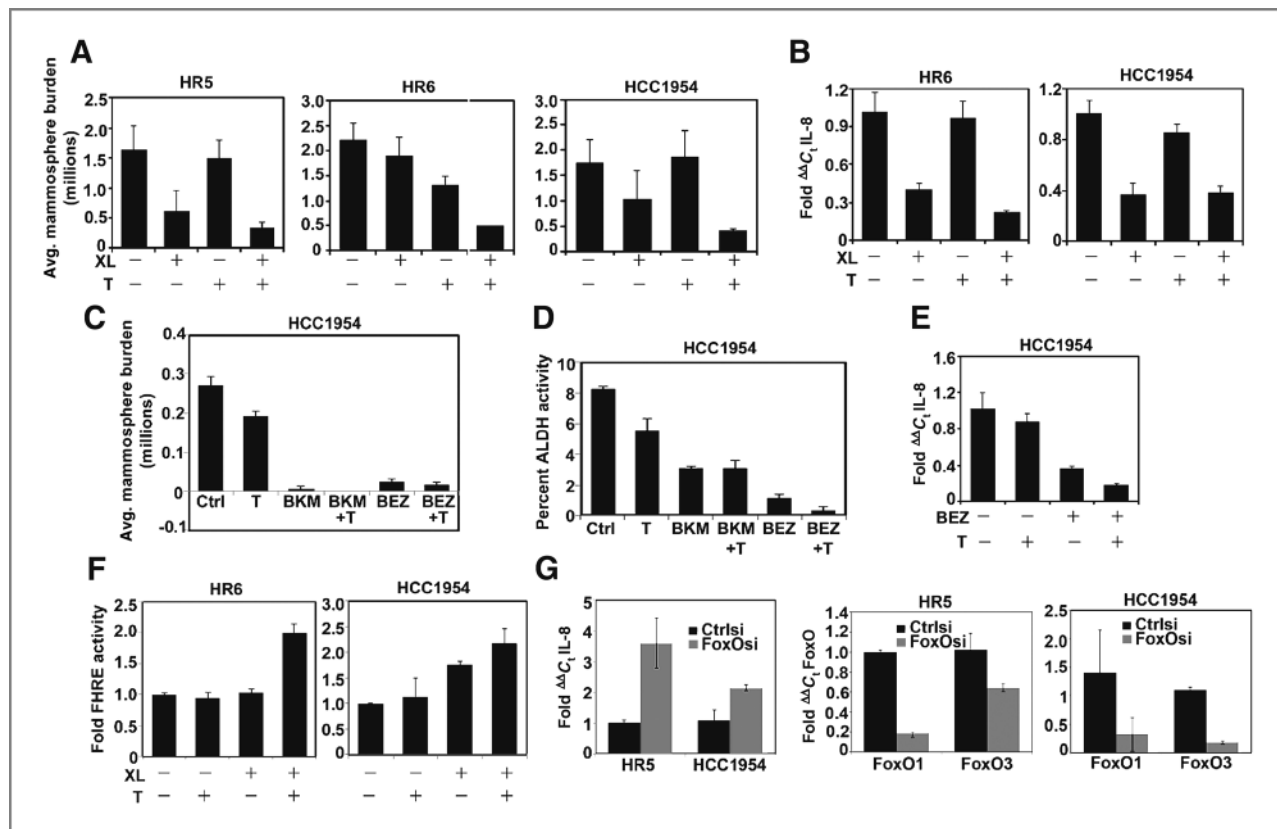


Figure 3. PI3K inhibition modulates the CSC fraction in trastuzumab-resistant cells. **A**, mammosphere assay was conducted with cells treated with 6 $\mu\text{mol/L}$ XL147, 10 $\mu\text{g/mL}$ trastuzumab, or both. Total mammosphere volume was measured on day 13 as described in Materials and Methods. Each bar represents mean \pm SD of 2 replicates. **B**, IL-8 qPCR was carried out on RNA isolated from HR6 and HCC1954 cells treated with XL147, trastuzumab, or XL147 + trastuzumab for 24 and 48 hours, respectively. Each bar represents mean \pm SE of triplicates. **C**, average mammosphere volume in HCC1954 cells treated with trastuzumab (10 $\mu\text{g/mL}$), BKM120 (1 $\mu\text{mol/L}$), BEZ235 (250 nmol/L), BKM120 + trastuzumab, or BEZ235 + trastuzumab for 7 days. Each bar represents mean \pm SE of 3 wells. **D**, percentage of ALDH activity in HCC1954 cells treated with the indicated inhibitors alone or in combination for 48 hours. Each bar represents mean \pm SD of duplicates. **E**, HCC1954 cells were treated with trastuzumab, BEZ235, or BEZ235 + trastuzumab for 48 hours before RNA isolation and subsequent IL-8 qPCR. Each bar represents the mean \pm SE of triplicates. **F**, luciferase activity was measured in HCC1954 and HR6 cells transiently transfected with a FoxO promoter-reporter (FHRE-Luc) and treated with DMSO, XL147 (6 $\mu\text{mol/L}$: HR6; 10 $\mu\text{mol/L}$: HCC1954), trastuzumab (10 $\mu\text{g/mL}$), or XL147 + trastuzumab. Each bar represents mean \pm SE of 6 replicates. **G**, HR5 and HCC1954 cells were transfected with control or FoxO1 and FoxO3 siRNA oligonucleotides as described previously (22). Three days later, the cells were harvested for RNA extraction followed by determination of IL-8, FoxO1, and 3 mRNA levels by qPCR. Each bar represents mean \pm SE of triplicates.

(Fig. 2D), suggesting the effect of XL147 on VEGF transcription was PI3K pathway-specific and not an off-target drug effect.

Treatment with PI3K inhibitor and trastuzumab reduces the drug-resistant CSC fraction

It has been proposed that the clinical efficacy of trastuzumab is due to its ability to target CSCs within trastuzumab-sensitive tumors (30, 31). CSC activity is studied *in vitro* by primary mammosphere formation (attachment-independent growth) and analysis of specific cell surface markers (32). ALDH positivity (ALDH+) correlates with HER2+ subtypes independent of estrogen receptor (ER) status (30, 33). More recently, the inflammatory cytokine IL-8 has also been directly associated with mammosphere formation and ALDH positivity in breast CSCs (34). Thus, we measured the sensitivity of the CSC fraction to combined inhibition of PI3K and HER2 by mammosphere formation, ALDH activity, and IL-8 expression. Treatment with trastuzumab alone reduced mammosphere

formation, ALDH activity, and IL-8 mRNA expression in trastuzumab-sensitive BT474 cells (Supplementary Fig. S3A). The trastuzumab-resistant HR5 and HR6 cell lines contained a higher proportion of CSCs as indicated by greater ability to form mammospheres, enhanced ALDH activity, and higher levels of IL-8 mRNA and protein (Supplementary Fig. S3B). In these cells, the combination of XL147 + trastuzumab reduced mammosphere formation (Fig. 3A), IL-8 mRNA (Fig. 3B), and ALDH activity (Supplementary Fig. S3C). Treatment of HCC1954 cells with BKM120 and BEZ235, each alone and in combination with trastuzumab, reduced mammosphere formation, ALDH activity, and IL-8 expression, suggesting the effects were specific to the PI3K pathway (Fig. 3C–E). Finally, RNAi of p110 α also reduced the CSC fraction in HCC1954 cells as measured by a decrease in mammosphere growth and ALDH activity (Supplementary Fig. S3E–S3G).

In epithelial and endothelial cells, FoxO1 and FoxO3 have been implicated as suppressors of IL-8 transcription (35, 36).

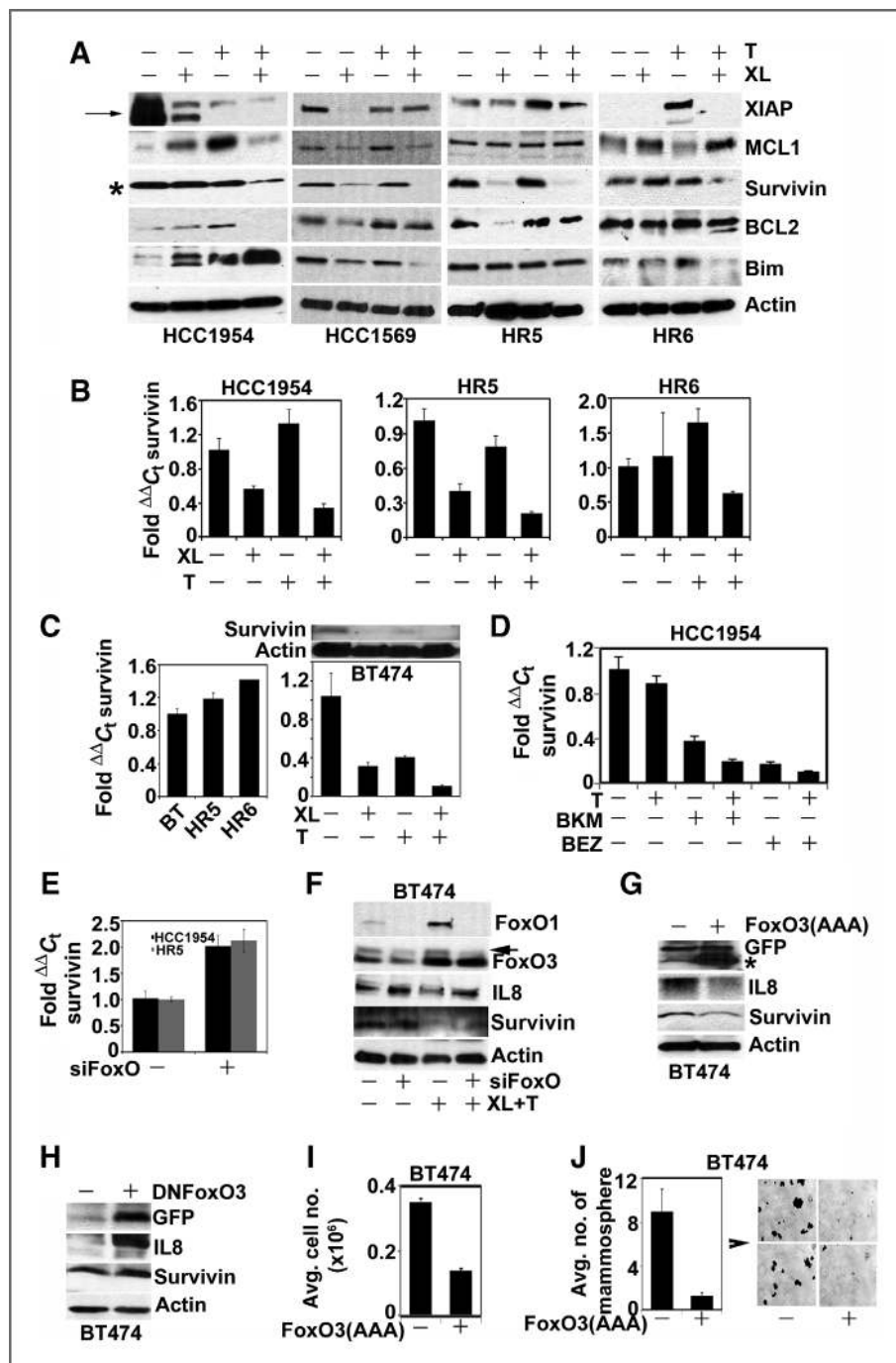


Figure 4. Combination of PI3K inhibitor and trastuzumab reduces survivin expression. **A** and **B**, cells were treated with XL147 (6 $\mu\text{mol/L}$), trastuzumab (10 $\mu\text{g/mL}$), or both inhibitors for 24 hours (HR6) or 48 hours (HR5, HCC1569, and HCC1954) and subjected to immunoblot analysis for pro- or antiapoptotic proteins (**A**) and qPCR for survivin mRNA (**B**). **B**, each bar represents the mean \pm SE of triplicates. **C**, survivin expression in trastuzumab-sensitive versus -resistant cells. Left, qPCR for survivin mRNA in BT474, HR5, and HR6; right, immunoblot (top) and qPCR (bottom) for survivin in BT474 cells treated with XL147, trastuzumab, or XL147 + trastuzumab for 48 hours. Each bar represents mean \pm SE of triplicates. **D**, qPCR for survivin mRNA in HCC1954 cells treated with trastuzumab, BKM120, BEZ235, BKM120 + trastuzumab, or BEZ235 + trastuzumab for 48 hours (same doses as in Fig. 3). Each bar represents mean \pm SE of triplicates. **E**, HR5 and HCC1954 cells were transfected with control or FoxO1 and FoxO3 siRNA duplexes for 3 days, followed by survivin qPCR. Each bar represents mean \pm SE of triplicates. **F**, BT474 cells were transfected with control or FoxO1 and FoxO3 siRNA duplexes and treated with 6 $\mu\text{mol/L}$ XL147 + 10 $\mu\text{g/mL}$ trastuzumab for 48 hours before immunoblot analyses. **G–J**, BT474 cells were infected with recombinant adenoviruses expressing GFP-tagged constitutively active FoxO3 (AAA; **G**, **I**, **J**) or dominant-negative DNFoxO3 (**H**). Control cells were infected with adenovirus encoding β -galactosidase/LacZ (Ad-CMV-b-Gal). **G** and **H**, six days postinfection, cells were harvested and lysates prepared for immunoblot analysis. **I**, eight days postinfection, cells were trypsinized and counted as indicated in Materials and Methods (each bar represents mean \pm SE of triplicates). **J**, twenty-four hours after infection, cells were plated in a mammosphere assay and imaged after 7 days (each bar represents mean \pm SE of triplicates; left). Mammospheres were dissociated by trypsin digestion and single cells were plated in monolayer in low density. After 7 days, tumor cell foci/colonies were stained with crystal violet and imaged with $\times 4$ magnification (right).

FoxO1 and FoxO3 activities are regulated by AKT-mediated phosphorylation. When AKT is inactive, FoxO factors are hypophosphorylated and predominantly nuclear where they modulate the transcription of target genes (37). We speculated that in trastuzumab-resistant cells, the combination of XL147 and trastuzumab, but not each drug alone, would optimally suppress PI3K-AKT resulting in FoxO-mediated suppression of IL-8 transcription. Indeed, the combination of XL147 and trastuzumab induced maximal activity of a FoxO3 promoter reporter transfected into HCC1954 and HR6 cells compared with each inhibitor alone (Fig. 3F). Furthermore, transfection of FoxO1 and FoxO3 siRNA duplexes into trastuzumab-resistant HR5 and HCC1954 cells resulted in a 2- and 3.5-fold upregulation of IL-8 mRNA, respectively (Fig. 3G).

Treatment with PI3K inhibitor and trastuzumab reduces survivin expression

To investigate mediators of the apoptosis induced by the combination of XL147 and trastuzumab in drug-resistant cells (Fig. 1C and D), we next examined levels of the proapoptotic molecule BIM and the antiapoptotic molecules X-linked inhibitor of apoptosis protein (XIAP), survivin, BCL2, and MCL1. By immunoblot analysis, only survivin, a member of the inhibitor of apoptosis/IAP family of antiapoptotic proteins (38), was downregulated in all cell lines upon treatment with XL147 + trastuzumab (Fig. 4A). Protein levels correlated with a change in survivin mRNA levels (Fig. 4B). Steady-state levels of survivin mRNA were similar between trastuzumab-sensitive (BT474) and -resistant (HR5 and HR6) cells (Fig. 4C, left; qPCR). However, in antibody-sensitive cells, treatment with trastuzumab inhibited survivin mRNA (qPCR) and protein (immunoblot) levels (Fig. 4C, right), whereas in the resistant cells, the antibody had no effect (Fig. 4A and B). In HCC1954 cells, BKM120 and BEZ235 each in combination with trastuzumab also reduced survivin mRNA levels (Fig. 4D), suggesting that survivin transcription is regulated by the PI3K pathway.

FoxO factors inhibit survivin gene transcription through direct interaction with its promoter (39, 40). Accordingly, siRNA knockdown of FoxO1 and FoxO3 in trastuzumab-resistant cells resulted in a 2-fold increase in survivin mRNA (Fig. 4E). Furthermore, in BT474 cells, RNAi of FoxO1/3 counteracted the XL147 + trastuzumab-mediated suppression of survivin protein levels (Fig. 4F). In addition, overexpression of a constitutively active mutant of FoxO3, where the 3 AKT phosphorylation sites had been substituted with Ala [FoxO3 (AAA)], reduced survivin protein levels (Fig. 4G) and BT474 cell growth and mammosphere formation (Fig. 4I and J). In a reverse experiment, transduction of a dominant-negative FoxO3, where the C-terminal transactivation domain has been deleted (dnFoxO3), resulted in a modest increase in survivin protein levels in BT474 cells (Fig. 4H). These data suggest that survivin expression is regulated by PI3K-FoxO in HER2-overexpressing breast cancer cells.

RNAi of FoxO1/3 partially rescued the reduction of IL-8 levels upon treatment with the combination of XL147 + trastuzumab (Fig. 4F). Conversely, BT474 cells transduced with

the constitutively active FoxO3 mutant exhibited reduced IL-8 expression (Fig. 4G), whereas dominant-negative FoxO3 had the opposite effect (Fig. 4H).

Downregulation of survivin restores sensitivity to trastuzumab

On the basis of the results shown in Fig. 4, we speculated that downregulation of survivin is required for the apoptosis induced by the combination of XL147 + trastuzumab in cells resistant to the antibody. Indeed, downregulation of survivin with RNAi (Fig. 5B) or with YM155, a small-molecule inhibitor of survivin transcription (41), in trastuzumab-resistant cells resulted in growth inhibition (Fig. 5A and C, top) and apoptosis (Fig. 5C, bottom and Supplementary Fig. S4A, B, and D). A second survivin siRNA oligonucleotide produced comparable levels of knockdown, apoptosis, and growth inhibition in HCC1954 cells (Supplementary Fig. S4E and S4F). Conversely, overexpression of survivin cDNA in drug-sensitive BT474 cells attenuated trastuzumab-mediated growth inhibition (Supplementary Fig. S4G).

Survivin has been reported to play a role in maintenance of CSCs (42, 43). Thus, we next tested whether genetic and/or pharmacologic inhibition of survivin would have an effect on the CSC fraction within trastuzumab-resistant cells. In HR5 and HCC1954 cells, RNAi-mediated knockdown of survivin decreased mammosphere formation; this was further reduced when the RNAi oligonucleotides were combined with trastuzumab (Fig. 5D). Treatment with YM155 alone or in combination with trastuzumab also reduced mammosphere formation (Fig. 5E). These effects correlated temporally with reduction in ALDH activity (Supplementary Fig. S4H and S4I).

Combination of PI3K inhibitor and trastuzumab inhibits growth of trastuzumab-resistant xenografts

On the basis of its superior ability to decrease survivin levels, we proposed that the combination of trastuzumab + XL147 would be a more potent inhibitor of trastuzumab-resistant xenograft growth compared with the PI3K inhibitor alone. Athymic mice bearing HR6 xenografts of ≥ 200 mm³ were randomized to therapy with vehicle, XL147, trastuzumab, or the combination of both inhibitors. Each drug alone modestly delayed HR6 tumor growth, whereas the combination of both inhibitors induced a marked antitumor effect (Fig. 6A). We next examined pharmacodynamic biomarkers of drug target inactivation after 28 days of treatment by immunohistochemistry (IHC), real-time qPCR (qRT-PCR), and immunoblot analyses. AKT activity has been shown to correlate directly with both cytoplasmic and nuclear levels of pAKT^{S473} (44). Consistent with the antitumor effect observed, only the combination of XL147 + trastuzumab reduced both cytoplasmic and nuclear pAKT levels (Fig. 6B, top). CD31 positivity (indicative of vessel formation/angiogenesis) and ALDH1 levels by IHC and IL-8 mRNA levels by qPCR were also lower in tumors treated with the combination (Figs. 6B, bottom, and D). Finally, only the combination reduced survivin levels as measured by immunoblot analysis of tumor lysates (Fig. 6C). These results were further verified in mice bearing HCC1954 xenografts treated with vehicle, trastuzumab, XL147, and the combination

of both drugs for 1 week. There was a noticeable decrease IL-8 and survivin expression (Supplementary Fig. S5) in tumors treated with the combination compared with tumors treated with each drug alone.

To support the clinical relevance of these data, we sought to determine whether steady-state and/or treatment-induced changes in survivin mRNA levels correlate with the response to trastuzumab in patients. In this study, patients with HER2⁺ breast cancer were treated with trastuzumab for 3 weeks, followed by a combination of trastuzumab + docetaxel for 12 weeks before surgery (45). Survivin mRNA was measured by microarray analysis in RNA extracted from tumor core biopsies obtained before therapy and from the surgical specimen after completion of the 4-month treatment. Evaluable matched microarray data were available in 13 patients. Five of 13 patients exhibited a response to treatment defined as absence

of any invasive cancer or only residual cancer of <0.1 cm in diameter in the surgical specimen (45). There was a significant reduction in survivin mRNA levels in the posttreatment compared with the pretreatment biopsies ($P = 0.0062$; Fig. 6E). Furthermore, pretreatment biopsies from patients exhibiting no response expressed significantly higher levels of survivin mRNA than those patients who responded clinically ($P = 0.026$; Fig. 6F) These data suggest that baseline levels and treatment-induced changes in survivin expression can potentially serve as a predictive biomarker of anti-HER2 therapy action in patients with HER2-overexpressing breast cancer.

Discussion

The antitumor action of trastuzumab depends, in part, on its ability to downregulate the PI3K/AKT signaling pathway.

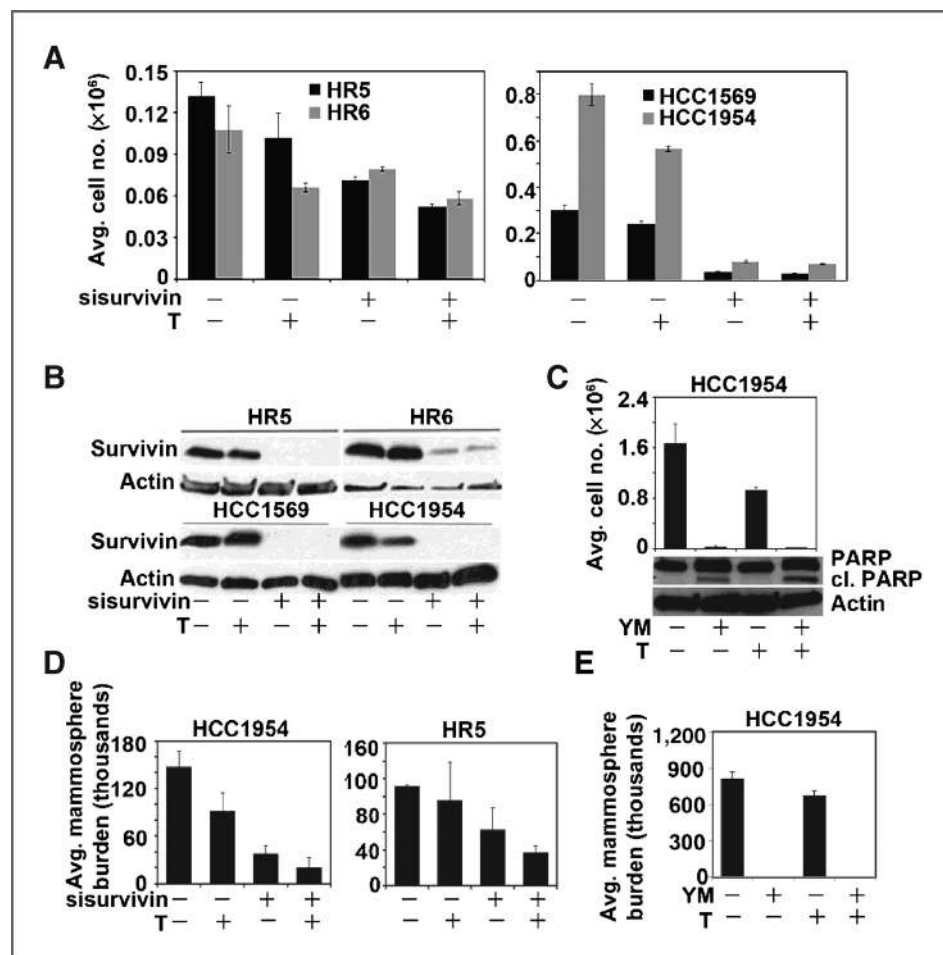


Figure 5. Downregulation of survivin restores sensitivity to trastuzumab. A, HR5 and HR6 (left) and HCC1569 and HCC1954 (right) cells were transfected with control or survivin siRNA duplexes and treated with 10 μ g/mL trastuzumab. Cells were counted after 6 (HR5 and HR6) or 4 (HCC1569 and HCC1954) days of treatment. Each bar represents mean \pm SE of 3 wells. B, immunoblot analysis of control or survivin siRNA-transfected cells \pm trastuzumab as indicated. C, growth inhibitory and proapoptotic effects of survivin transcriptional inhibitor in HCC1954 cells. Cells were treated with YM155 (50 nmol/L), trastuzumab (10 μ g/mL), or both inhibitors and harvested for cell counting on day 5 (top) or immunoblot analysis for PARP cleavage after 24 hours (bottom). Each bar represents mean \pm SE of triplicates. D and E, effects of survivin knockdown with either siRNA (D) or YM155 (E) on CSCs within trastuzumab-resistant cells. D, average mammosphere volume in HCC1954 and HR5 cells transfected with control or survivin siRNA and treated with trastuzumab for 6 days. Each bar represents mean \pm SD of duplicates. E, average mammosphere volume in HCC1954 cells treated with YM155, trastuzumab, or YM155 + trastuzumab for 6 days. Each bar represents mean \pm SE of triplicates.

Persistent activation of this pathway has been shown to confer resistance to trastuzumab (reviewed in ref. 8). Despite the increasing availability of therapeutic inhibitors of the PI3K/AKT/TOR pathway (reviewed in ref. 14) and abundant pre-clinical data linking this pathway with drug resistance, few mechanistic studies have examined the role of these inhibitors in trastuzumab-resistant breast cancer cells. We report here in the cellular, biochemical, and molecular effects of the ATP-competitive, reversible PI3K inhibitor XL147 against a panel of trastuzumab-resistant breast cancer cell lines and xenografts. The superior antiproliferative and antitumor action of XL147 in combination with trastuzumab concurred with its ability to promote cell death and cell-cycle arrest (Figs. 1 and 6A) and reduce AKT phosphorylation both *in vitro* (Fig. 2A) and *in vivo* (Fig. 6B).

HER2/PI3K/AKT signaling potentially induces expression of the proangiogenic factor VEGF (2). Treatment with trastuzumab reduces tumor VEGF *in vivo*, and this effect has been proposed to be central to the antitumor action of the antibody

against HER2-dependent xenografts (26). We observed that in drug-resistant xenografts, the combination of XL147 and trastuzumab reduced VEGF protein content and RNA expression, VEGF receptor phosphorylation, and blood vessel formation more potently than each drug alone (Figs. 2B–D and 6B), suggesting that PI3K-dependent enhanced angiogenesis is associated with resistance to trastuzumab.

Metastatic tumor relapses are characterized by rapidly proliferating, drug-resistant cancers associated with a high mortality rate. An increasing body of evidence suggests that survival of a small population of cells with stem-like properties may be responsible for these tumor recurrences after an initial response to anticancer therapy. This population, interchangeably called CSCs or "tumor-initiating cells" (TIC), retains the capacity to self-renew and regenerate the total bulk of a heterogeneous tumor comprised mostly of non-stem cells. Therefore, to achieve cures, both CSCs and non-CSCs within a given tumor should be eliminated (46). It has been proposed that in HER2⁺ tumors, PI3K/AKT signaling increases the CSC

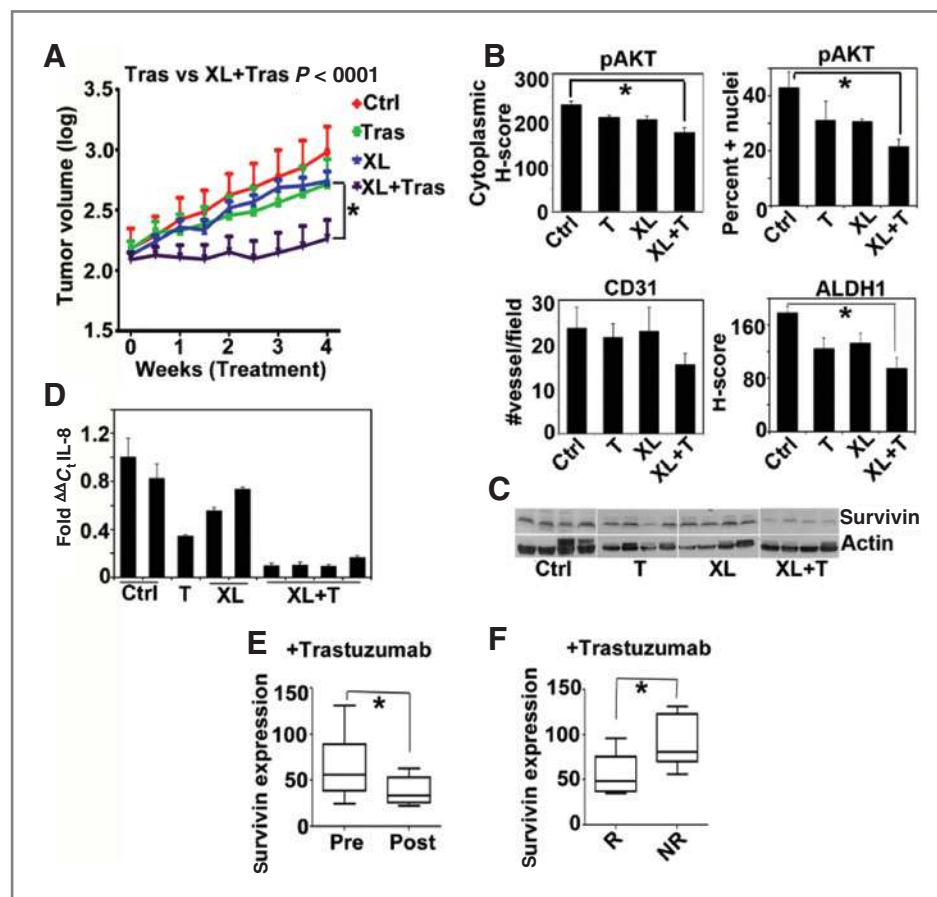


Figure 6. PI3K inhibitor + trastuzumab inhibit growth of trastuzumab-resistant xenografts. **A**, volumes of HR6 xenografts established in athymic mice treated with vehicle (Ctrl), XL147, trastuzumab, or XL147 + trastuzumab. Each data point represents the log-transformed value of mean tumor volume \pm SE over the time indicated in the x-axis. **B**, *H*-score analysis of IHC sections for pAKT^{S473}, CD31, and ALDH1. Each bar represents mean \pm SE. *, $P < 0.05$, unpaired *t* test. **C**, immunoblot analysis for survivin expression in tumor lysates collected on day 28. **D**, qPCR analysis for IL-8 mRNA in HR6 xenografts harvested on day 28. Each bar represents mean \pm SE of 3 wells. **E** and **F**, survivin mRNA expression in 13 HER2⁺ paired breast tumors from patients treated with neoadjuvant trastuzumab + chemotherapy as described in Results. **E**, comparison between the pre- and posttreatment survivin RNA levels in primary tumor biopsies. Each bar represents mean \pm SE ($n = 13$). *, $P < 0.05$; paired *t* test. **F**, survivin mRNA levels in pretreatment biopsies of tumors that responded (R) versus those who did not respond (NR) to neoadjuvant trastuzumab. Each bar represents mean \pm SE. *, $P < 0.05$; Mann-Whitney test.

fraction required for tumor progression (30). Indeed, treatment with trastuzumab reduced the CSC fraction in drug-sensitive BT474 cells (Supplementary Fig. S3A) and xenografts (Fig. 6B). Conversely, this was not observed in antibody-resistant HR5, HR6, and HCC1954 cells (Fig. 3 and Supplementary Fig. S3C). However, treatment with the PI3K inhibitor and trastuzumab reduced CSCs in trastuzumab-resistant tumors (Figs. 3 and 6B and Supplementary Fig. S3C–S3G) while decreasing expression of IL-8, a cytokine that depends on FoxO transcription factors (Figs. 3B and G, 4F–H, and 6D) and that promotes maintenance of CSCs (47). These data suggest that the reduction of CSCs is associated with restoration of sensitivity to the anti-HER2 therapy.

Cell death induced by anticancer therapies is triggered by drug-induced modulation of endogenous levels of pro- and antiapoptotic proteins. In the case of anti-HER2 therapies, this is the result of drug-induced downregulation of the PI3K/AKT and RAS/MEK/ERK pathways (48). The proapoptotic effects of the combination of XL147 and trastuzumab in trastuzumab-resistant cells and xenografts correlated temporally with transcriptional inhibition of survivin, a member of the IAP family. High survivin expression has been associated with high nuclear grade, negative hormone receptor status, HER2 and VEGF overexpression, and worse disease-free or overall survival in breast cancer (49). In this study, inhibition of survivin function with either siRNA or a small-molecule inhibitor reduced CSCs and non-CSCs in trastuzumab-resistant cells (Fig. 5 and Supplementary Fig. S4), further suggesting a causal association of survivin expression with drug resistance. Similar to the effect on IL-8, the transcriptional repression of survivin also depended on FoxO factors (Fig. 4). Finally, high levels of survivin mRNA in HER2⁺ tumors correlated with a poor clinical response to trastuzumab-containing neoadjuvant therapy (Fig. 6F). These data suggest that in HER2⁺ tumors with high levels of survivin, a more sustained and comprehensive inhibition of the HER2/PI3K axis, perhaps with the addition of a PI3K pathway inhibitor, will be required to suppress expres-

sion of this antiapoptotic protein. In sum, we conclude that acquired resistance to anti-HER2 therapies and subsequent metastatic progression of HER2-overexpressing cancers can be significantly ameliorated by early combinations of drugs that simultaneously target the HER2 receptor and the PI3K pathway.

Disclosure of Potential Conflicts of Interest

No potential conflicts of interest were disclosed.

Authors' Contributions

Conception and design: A. Chakrabarty, J.C. Chang

Development of methodology: A. Chakrabarty, C.L. Arteaga

Acquisition of data (provided animals, acquired and managed patients, provided facilities, etc.): N.E. Bhola, C.R. Sutton, R. Ghosh, M.G. Kuba, J.C. Chang

Analysis and interpretation of data (e.g., statistical analysis, biostatistics, computational analysis): A. Chakrabarty, N.E. Bhola, C.R. Sutton, R. Ghosh, B. Dave

Writing, review, and/or revision of the manuscript: A. Chakrabarty, J.C. Chang, C.L. Arteaga

Administrative, technical, or material support (i.e., reporting or organizing data, constructing databases): C.R. Sutton

Study supervision: A. Chakrabarty, C.L. Arteaga

Other: Carried out experiments, A. Chakrabarty

Grant Support

C.L. Arteaga is supported by a Stand Up To Cancer Dream Team Translational Research Grant, a Program of the Entertainment Industry Foundation (SU2C-AACR-DT0209). This work was supported by R01 grant CA80195 (C.L. Arteaga), ACS Clinical Research Professorship Grant CRP-07-234, Lee Jeans Translational Breast Cancer Research Program, Susan G. Komen for the Cure Foundation Grant SAC100013, Breast Cancer Specialized Program of Research Excellence grant P50 CA98131, and Vanderbilt-Ingram Cancer Center Support grant P30 CA68485. A. Chakrabarty and R. Ghosh are supported by post-doctoral fellowships from the Susan G. Komen for the Cure Foundation (KG091215) and DOD Breast Cancer Research program (W81XWH-09-1-0474), respectively.

The costs of publication of this article were defrayed in part by the payment of page charges. This article must therefore be hereby marked *advertisement* in accordance with 18 U.S.C. Section 1734 solely to indicate this fact.

Received June 25, 2012; revised October 9, 2012; accepted November 11, 2012; published OnlineFirst November 29, 2012.

References

- Olayioye MA, Neve RM, Lane HA, Hynes NE. The ErbB signaling network: receptor heterodimerization in development and cancer. *EMBO J* 2000;19:3159–67.
- Moasser MM. The oncogene HER2: its signaling and transforming functions and its role in human cancer pathogenesis. *Oncogene* 2007;26:6469–87.
- Slamon DJ, Clark GM, Wong SG, Levin WJ, Ullrich A, McGuire WL. Human breast cancer: correlation of relapse and survival with amplification of the HER-2/neu oncogene. *Science* 1987;235:177–82.
- Holbro T, Beerli RR, Maurer F, Koziczak M, Barbas CF III, Hynes NE. The ErbB2/ErbB3 heterodimer functions as an oncogenic unit: ErbB2 requires ErbB3 to drive breast tumor cell proliferation. *Proc Natl Acad Sci U S A* 2003;100:8933–8.
- Lee-Hoeflich ST, Crocker L, Yao E, Pham T, Munroe X, Hoeflich KP, et al. A central role of HER3 in HER2-amplified breast cancer: implications for targeted therapy. *Cancer Res* 2008;68:5878–87.
- Yakes FM, Chinratanalab W, Ritter CA, King W, Seelig S, Arteaga CL. Herceptin-induced inhibition of phosphatidylinositol-3 kinase and AKT is required for antibody-mediated effects on p27, Cyclin D1, and antitumor action. *Cancer Res* 2002;62:4132–41.
- Carter P, Presta L, Gorman CM, Ridgway JB, Henner D, Wong WL, et al. Humanization of an anti-p185HER2 antibody for human cancer therapy. *Proc Natl Acad Sci U S A* 1992;89:4285–9.
- Stern HM. Improving treatment of HER2-positive cancers: opportunities and challenges. *Sci Transl Med* 2012;4:127rv2.
- Nahta R, Esteva FJ. Trastuzumab: triumphs and tribulations. *Oncogene* 2007;26:3637–43.
- Nagata Y, Lan K-H, Zhou X, Tan M, Esteva FJ, Sahin AA, et al. PTEN activation contributes to tumor inhibition by trastuzumab, and loss of PTEN predicts trastuzumab resistance in patients. *Cancer Cell* 2004;6:117–27.
- Kataoka Y, Mukohara T, Shimada H, Saijo N, Hirai M, Minami H. Association between gain-of-function mutations in *PIK3CA* and resistance to HER2-targeted agents in *HER2*-amplified breast cancer cell lines. *Ann Oncol* 2010;21:255–62.
- Eichhorn PJ, Gili M, Scaltriti M, Serra V, Guzman M, Nijkamp W, et al. Phosphatidylinositol 3-kinase hyperactivation results in lapatinib resistance that is reversed by the mTOR/phosphatidylinositol 3-kinase inhibitor NVP-BE235. *Cancer Res* 2008;68:9221–30.
- Junttila TT, Akita RW, Parsons K, Fields C, Phillips GDL, Friedman LS, et al. Ligand-independent HER2/HER3/PI3K complex is disrupted by

- trastuzumab and is effectively inhibited by the PI3K inhibitor GDC-0941. *Cancer Cell* 2009;15:429–40.
14. Tsang RY, Finn RS. Beyond trastuzumab: novel therapeutic strategies in HER2-positive metastatic breast cancer. *Br J Cancer* 2012;106:6–13.
 15. Edelman G, Bedell C, Shapiro G, Pandya SS, Kwak EL, Scheffold C, et al. A phase I dose-escalation study of XL147 (SAR245408), a PI3K inhibitor administered orally to patients (pts) with advanced malignancies. *J Clin Oncol* 2010;28:3004.
 16. McDermott SP, Wicha MS. Targeting breast cancer stem cells. *Mol Oncol* 2010;4:404–19.
 17. Ritter CA, Perez-Torres M, Rinehart C, Guix M, Dugger T, Engelman JA, et al. Human breast cancer cells selected for resistance to trastuzumab *in vivo* overexpress epidermal growth factor receptor and ErbB ligands and remain dependent on the ErbB receptor network. *Clin Cancer Res* 2007;13:4909–19.
 18. Brunet A, Bonni A, Zigmond MJ, Lin MZ, Juo P, Hu LS, et al. Akt promotes cell survival by phosphorylating and inhibiting a Forkhead transcription factor. *Cell* 1999;96:857–68.
 19. Wang SE, Narasanna A, Perez-Torres M, Xiang B, Wu FY, Yang S, et al. HER2 kinase domain mutation results in constitutive phosphorylation and activation of HER2 and EGFR and resistance to EGFR tyrosine kinase inhibitors. *Cancer Cell* 2006;10:25–38.
 20. Balko JM, Miller TW, Morrison MM, Hutchinson K, Young C, Rinehart C, et al. The receptor tyrosine kinase ErbB3 maintains the balance between luminal and basal breast epithelium. *Proc Natl Acad Sci U S A* 2012;109:221–6.
 21. Chakrabarty A, Rexer BN, Wang SE, Cook RS, Engelman JA, Arteaga CL. H1047R phosphatidylinositol 3-kinase mutant enhances HER2-mediated transformation by heregulin production and activation of HER3. *Oncogene* 2010;29:5193–203.
 22. Chakrabarty A, Sanchez V, Kuba MG, Rinehart C, Arteaga CL. Feedback upregulation of HER3 (ErbB3) expression and activity attenuates antitumor effect of PI3K inhibitors. *Proc Natl Acad Sci USA* 2012;109:2718–23.
 23. Allen LF, Sebolt-Leopold J, Meyer MB. CI-1040 (PD184352), a targeted signal transduction inhibitor of MEK (MAPKK). *Semin Oncol* 2003;30:105–16.
 24. Weigelt B, Warne PH, Downward J. PIK3CA mutation, but not PTEN loss of function, determines the sensitivity of breast cancer cells to mTOR inhibitory drugs. *Oncogene* 2011;30:3222–33.
 25. Chandralapaty S, Sawai A, Scaltriti M, Rodrik-Outmezguine V, Grbovic-Huezo O, Serra V, et al. AKT inhibition relieves feedback suppression of receptor tyrosine kinase expression and activity. *Cancer Cell* 2011;19:58–71.
 26. Izumi Y, Xu L, di Tomaso E, Fukumura D, Jain RK. Tumour biology: herepentin acts as an anti-angiogenic cocktail. *Nature* 2002;416:279–80.
 27. Karadedou CT, Gomes AR, Chen J, Petkovic M, Ho KK, Zwolinska AK, et al. FOXO3a represses VEGF expression through FOXM1-dependent and -independent mechanisms in breast cancer. *Oncogene* 2012;31:1845–58.
 28. Voliva CF, Pecchi S, Burger M, Nagel T, Schnell C, Fritsch C, et al. Biological characterization of NVP-BKM120, a novel inhibitor of phosphoinositide 3-kinase in Phase I/II clinical trials [abstract]. In: Proceedings of the 101st Annual Meeting of the American Association for Cancer Research; 2010 Apr 17–21; Washington, DC. Philadelphia (PA): AACR; 2010. Abstract no. 4498, poster session: 25, session category: Experimental and Molecular Therapeutics 34.
 29. Maira SM, Stuffer F, Brueggen J, Furet P, Schnell C, Fritsch C, et al. Identification and characterization of NVP-BE2255, a new orally available dual phosphatidylinositol 3-kinase/mammalian target of rapamycin inhibitor with potent *in vivo* antitumor activity. *Mol Cancer Ther* 2008;7:1851–63.
 30. Korkaya H, Paulson A, Iovino F, Wicha MS. HER2 regulates the mammary stem/progenitor cell population driving tumorigenesis and invasion. *Oncogene* 2008;27:6120–30.
 31. Magnifico A, Albano L, Campaner S, Delia D, Castiglioni F, Gasparini P, et al. Tumor-initiating cells of HER2-positive carcinoma cell lines express the highest oncoprotein levels and are sensitive to trastuzumab. *Clin Cancer Res* 2009;15:2010–21.
 32. Nakshatri H, Srour E, Badve S. Breast cancer stem cells and intrinsic subtypes: controversies rage on. *Curr Stem Cell Res Ther* 2009;4:50–60.
 33. Ginestier C, Hur MH, Charafe-Jauffret E, Monville F, Dutcher J, Brown M, et al. ALDH1 is a marker of normal and malignant human mammary stem cells and a predictor of poor clinical outcome. *Cell Stem Cell* 2007;1:555–67.
 34. Charafe-Jauffret E, Ginestier C, Iovino F, Wicinski J, Cervera N, Finetti P, et al. Breast cancer cell lines contain functional cancer stem cells with metastatic capacity and a distinct molecular signature. *Cancer Res* 2009;69:1302–13.
 35. Potente M, Urbich C, Sasaki K, Hofmann WK, Heeschen C, Aicher A, et al. Involvement of Foxo transcription factors in angiogenesis and postnatal neovascularization. *J Clin Invest* 2005;115:2382–92.
 36. Snoeks L, Weber CR, Turner JR, Bhattacharyya M, Wasland K, Savkovic SD. Tumor suppressor Foxo3a is involved in the regulation of lipopolysaccharide-induced interleukin-8 in intestinal HT-29 cells. *Infect Immun* 2008;76:4677–85.
 37. Myatt SS, Lam EW-F. The emerging roles of forkhead box (Fox) proteins in cancer. *Nat Rev Cancer* 2007;7:847–59.
 38. Altieri DC. Survivin, cancer networks and pathway-directed drug discovery. *Nat Rev Cancer* 2008;8:61–70.
 39. Guha M, Plescia J, Leav I, Li J, Languino LR, Altieri DC. Endogenous tumor suppression mediated by PTEN involves survivin gene silencing. *Cancer Res* 2009;69:4954–8.
 40. Obexer P, Hagenbuchner J, Unterkircher T, Sachsenmaier N, Seifarth C, Bock G, et al. Repression of BIRC5/survivin by FOXO3/FKHRL1 sensitizes human neuroblastoma cells to DNA damage-induced apoptosis. *Mol Biol Cell* 2009;20:2041–8.
 41. Nakahara T, Kita A, Yamanaka K, Mori M, Amino N, Takeuchi M, et al. Broad spectrum and potent antitumor activities of YM155, a novel small-molecule survivin suppressant, in a wide variety of human cancer cell lines and xenograft models. *Cancer Sci* 2011;102:614–21.
 42. Lee CW, Simin K, Liu Q, Plescia J, Guha M, Khan A, et al. A functional Notch-survivin gene signature in basal breast cancer. *Breast Cancer Res* 2008;10:R97.
 43. Leung CG, Xu Y, Mularski B, Liu H, Gurbuxani S, Crispino JD. Requirements for survivin in terminal differentiation of erythroid cells and maintenance of hematopoietic stem and progenitor cells. *J Exp Med* 2007;204:1603–11.
 44. Martelli AM, Faenza I, Billi AM, Manzoli L, Evangelisti C, Falà F, et al. Intracellular 3'-phosphoinositide metabolism and Akt signaling: new mechanisms for tumorigenesis and protection against apoptosis? *Cell Signal* 2006;18:1101–7.
 45. Dave B, Migliaccio I, Gutierrez MC, Wu M-F, Chamness GC, Wong H, et al. Loss of phosphatase and tensin homolog or phosphoinositide-3 kinase activation and response to trastuzumab or lapatinib in human epidermal growth factor receptor 2-overexpressing locally advanced breast cancers. *J Clin Oncol* 2011;29:166–73.
 46. Diehn M, Cho RW, Clarke MF. Therapeutic implications of the cancer stem cell hypothesis. *Semin Radiat Oncol* 2009;19:78–86.
 47. Ginestier C, Liu S, Diebel ME, Korkaya H, Luo M, Brown M, et al. CXCR1 blockade selectively targets human breast cancer stem cells *in vitro* and in xenografts. *J Clin Invest* 2010;120:485–97.
 48. Faber AC, Li D, Song Y, Liang MC, Yeap BY, Bronson RT, et al. Differential induction of apoptosis in HER2 and EGFR addicted cancers following PI3K inhibition. *Proc Natl Acad Sci U S A* 2009;106:19503–8.
 49. Ryan BM, Konecny GE, Kahlert S, Wang HJ, Untch M, Meng G, et al. Survivin expression in breast cancer predicts clinical outcome and is associated with HER2, VEGF, urokinase plasminogen activator and PAI-1. *Ann Oncol* 2006;17:597–604.

Cancer Research

The Journal of Cancer Research (1916–1930) | The American Journal of Cancer (1931–1940)

Trastuzumab-Resistant Cells Rely on a HER2-PI3K-FoxO-Survivin Axis and Are Sensitive to PI3K Inhibitors

Anindita Chakrabarty, Neil E. Bhola, Cammie Sutton, et al.

Cancer Res 2013;73:1190-1200. Published OnlineFirst November 29, 2012.

Updated version Access the most recent version of this article at:
doi:[10.1158/0008-5472.CAN-12-2440](https://doi.org/10.1158/0008-5472.CAN-12-2440)

Supplementary Material Access the most recent supplemental material at:
<http://cancerres.aacrjournals.org/content/suppl/2012/11/29/0008-5472.CAN-12-2440.DC1>

Cited articles This article cites 48 articles, 20 of which you can access for free at:
<http://cancerres.aacrjournals.org/content/73/3/1190.full#ref-list-1>

Citing articles This article has been cited by 13 HighWire-hosted articles. Access the articles at:
<http://cancerres.aacrjournals.org/content/73/3/1190.full#related-urls>

E-mail alerts [Sign up to receive free email-alerts](#) related to this article or journal.

Reprints and Subscriptions To order reprints of this article or to subscribe to the journal, contact the AACR Publications Department at pubs@aacr.org.

Permissions To request permission to re-use all or part of this article, use this link
<http://cancerres.aacrjournals.org/content/73/3/1190>.
Click on "Request Permissions" which will take you to the Copyright Clearance Center's (CCC) Rightslink site.